The Journal of Chemical Physics

Reproducibility of cavity-enhanced chemical reaction rates in the vibrational strong coupling regime

Cite as: J. Chem. Phys. **154**, 191103 (2021); https://doi.org/10.1063/5.0046307
Submitted: 02 February 2021 • Accepted: 29 April 2021 • Published Online: 18 May 2021

Mario V. Imperatore, John B. Asbury and Noel C. Giebink

The Journal of Chemical Physics COMMUNICATION scitation.org/journal/jcp

Reproducibility of cavity-enhanced chemical reaction rates in the vibrational strong coupling regime

Cite as: J. Chem. Phys. 154, 191103 (2021); doi: 10.1063/5.0046307
Submitted: 2 February 2021 • Accepted: 29 April 2021 •
Published Online: 18 May 2021

Mario V. Imperatore,[1] John B. Asbury,[2] and Noel C. Giebink[1,a)]

AFFILIATIONS

[1] Department of Electrical Engineering, The Pennsylvania State University, University Park, Pennsylvania 16802, USA
[2] Department of Chemistry, The Pennsylvania State University, University Park, Pennsylvania 16802, USA

Note: This paper is part of the JCP Special Topic on Polariton Chemistry: Molecules in Cavities and Plasmonic Media.
[a)] **Author to whom correspondence should be addressed:** ncg2@psu.edu

ABSTRACT

One of the most exciting and debated aspects of polariton chemistry is the possibility that chemical reactions can be catalyzed by vibrational strong coupling (VSC) with confined optical modes in the absence of external illumination. Here, we report an attempt to reproduce the enhanced rate of cyanate ion hydrolysis reported by Hiura *et al.* [chemRxiv:7234721 (2019)] when the collective OH stretching vibrations of water (which is both the solvent and a reactant) are strongly coupled to a Fabry–Pérot cavity mode. Using a piezo-tunable microcavity, we reproduce the reported vacuum Rabi splitting but fail to observe any change in the reaction rate as the cavity thickness is tuned in and out of the strong coupling regime during a given experiment. These findings suggest that there are subtleties involved in successfully realizing VSC-catalyzed reaction kinetics and therefore motivate a broader effort within the community to validate the claims of polariton chemistry in the dark.

I. INTRODUCTION

The emerging field of polariton chemistry[1–5] is based on the notion that strong coupling molecular electronic or vibrational transitions to an optical microcavity mode can alter the rate or yield of a chemical reaction. While there is growing experimental[6–10] and theoretical[11–16] evidence to support such cavity modification of photochemical reactions initiated by external illumination, the most striking observation so far is that certain reactions appear to be altered even in the dark when their reactant,[17–21] product,[17] or solvent[19,20,22] molecules exist in the vibrational strong coupling (VSC) regime.

These observations are puzzling at first glance since the majority of molecules in a typical planar microcavity experiment are thought to remain uncoupled (although recent work has shown that dark states in the cavity do delocalize to some extent[23–25]) and thus would seem to dominate the ensemble-level reaction thermodynamics.[26,27] Significant theoretical effort[26–31] has consequently been devoted to understanding the mechanism(s) underlying the many dark reaction changes that have been reported; however, there have been surprisingly a few published attempts to independently reproduce and validate the findings of the original experiments as part of the normal scientific process.

Here, we report our attempt to reproduce the ~ 100-fold acceleration of cyanate ion hydrolysis, $2H_2O + OCN^- \rightarrow CO_3^{2-} + NH_4^+$, which was reported by Hiura *et al.*[20] when the collective OH stretching vibrations of water (which acts both as a solvent and a reactant) are strongly coupled to a Fabry–Pérot cavity mode. Using a piezo-tunable microcavity, we reproduce the ~800 cm^{-1} vacuum Rabi splitting achieved in Ref. 20 but do not observe any change in the reaction rate when the cavity is tuned in and out of the VSC regime. These results suggest that as-yet-unappreciated experimental factors may play a pivotal role in achieving VSC control over chemical reactions in the dark.

II. EXPERIMENTAL

Potassium cyanate (KOCN, 97%) is purchased from ACROS Organics™ and used as received with ultrapure water (ARISTAR® ULTRA) purchased from VWR Chemicals BDH®. Following

Ref. 20, we infer the progress of the hydrolysis reaction from the change in the cyanate ion concentration over time as determined from the absorbance of its asymmetric stretching mode at 2169 cm^{-1}. Transmission measurements are collected from microcavity samples at normal incidence using a JASCO FT/IR-6600 FTIR spectrometer and from non-cavity samples via attenuated total internal reflection (ATR) of unpolarized light at an incidence angle of 45° using a Ge ATR crystal on a Bruker VERTEX 70v FTIR spectrometer with a Harrick Seagull variable angle reflection accessory.

Similar to Ref. 32, actively tunable microcavities are constructed from 25.4 mm-diameter sapphire optical windows with λ flatness (WG31050, Thorlabs), one of which is mounted on a piezo-controlled translation stage that enables manual movement over a 5 mm range with 1 μm resolution and piezoelectric actuation over a 20 μm range with 0.6 nm resolution. The entire setup is built on a small breadboard that can be inserted into the FTIR sample chamber as illustrated in Fig. 1(a). Gold mirrors are deposited by e-beam evaporation with an approximate thickness of 10 nm at 0.5 Å/s on top of a 1.5 nm-thick Ge wetting layer to minimize surface roughness.[33] As in Ref. 20, a ~ 100 nm-thick layer of SiO_2 is deposited (also via e-beam evaporation) on top of the Au to avoid direct contact between the metal and solution.

After placing the sapphire windows in their kinematic mounts, they are interferometrically aligned in three steps to achieve the high degree of parallelism required to actuate a few-micron-thick cavity with macroscopic dimensions. First, the mirrors are coarsely set parallel by observing the walk-off in multiple reflections of a HeNe laser beam. Next, the same beam is expanded, and the mirror tilts

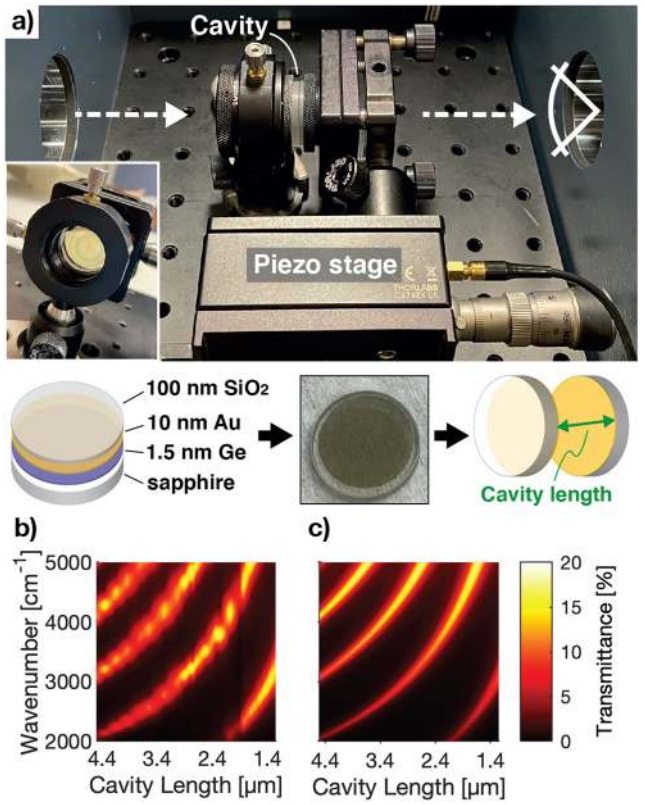

FIG. 1. (a) Schematic of the cavity measurement setup. The cavity consists of two sapphire windows that are coated with Ge/Au/SiO_2 mirrors as shown in the lower illustration. One of the windows is fixed, while the other is mounted on a piezo-controlled translation stage to actively control the cavity thickness. When the cavity is aligned, concentric Newton rings are visible (lower left inset); the extent of the central fringe confirms a negligible ($< \lambda/4$) thickness variation across the center of the cavity probed by the FTIR beam. Cavity catalysis experiments are conducted by infiltrating aqueous KOCN solution between the windows via capillary action. (b) Transmission spectrum measured for an empty (i.e., air-spaced) cavity as a function of its thickness. (c) Transfer matrix simulation of the cavity transmittance based on layer thicknesses and optical constants determined by ellipsometry.

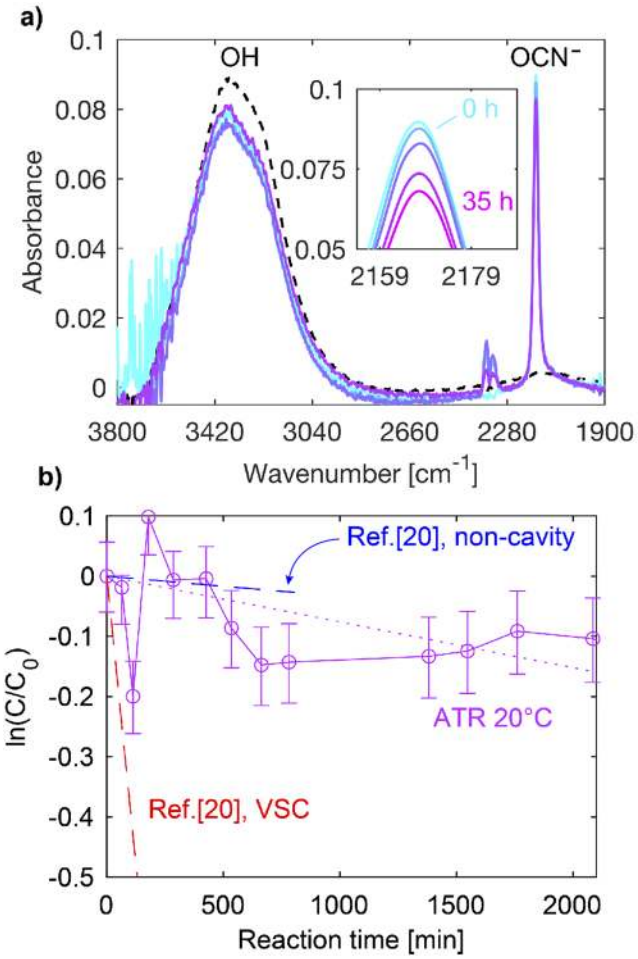

FIG. 2. (a) Absorbance spectra of a 2 mol/l aqueous KOCN solution measured via ATR over the course of 35 h; the temperature of the solution is maintained at 20° C over this time period. The inset provides an expanded view of the changing OCN^- peak at 2169 cm^{-1} and the black dashed line shows the absorbance of pure water for reference; the small peaks with variable amplitude near 2350 cm^{-1} are associated with residual CO_2 in the FTIR sample chamber. (b) Time dependence of the OCN^- peak (purple circles). The purple dashed line is a fit to determine the hydrolysis reaction rate; the dashed blue and red lines show the results from Ref. 20 for comparison. Error bars are derived by propagating the standard deviation of multiple independent ATR measurements at each time point.

are adjusted until the transmitted interference fringes form concentric circles. This corresponds to the formation of Newton rings under room light illumination, which provide a clear visual indication that the thickness variation across the central region of the cavity probed by the ~ 10 mm diameter FTIR beam is less than ~ 150 nm [i.e., a quarter wave in the visible region; see the inset of Fig. 1(a)]. The fringe pattern is then monitored as the cavity thickness is decreased to the desired value, and the entire breadboard apparatus is carefully placed into the FTIR sample chamber and purged with dry N_2.

Figure 1(b) shows the normal incidence transmission spectrum of a typical empty (i.e., air-spaced) cavity as its thickness is varied over the range 1.4–4.4 μm. The transmission maxima track the dispersion of the m = 1–4 Fabry–Pérot modes and are well reproduced in the transfer matrix simulation[34] shown in Fig. 1(c). The linewidth of the experimental cavity modes is broader than the transfer matrix simulation (the finesse measured for a 3 μm-thick cavity is $F \sim 5$) due to the variation in cavity thickness over the FTIR beam spot, which is evident from the Newton rings in the inset of Fig. 1(a). Cavities made using flatter ($\lambda/4$) CaF_2 optical windows with the same Au mirrors achieve a finesse that is roughly two times higher as shown in the supplementary material.

Cavity catalysis measurements are carried out by mixing KOCN and ultra-pure water in sterile vials that have been previously cleaned with methanol or isopropanol and rinsed with deionized water. We target the same 1:25 KOCN:H_2O molar ratio (2 mol/l concentration) employed by Hiura *et al.*[20] by dissolving 1.921 g of KOCN in 10.884 ml of water. Each solution is stirred for 5 min and then introduced inside a pre-aligned cavity by opening the sandwich and placing a drop in the center. We then adjust the cavity length to the desired value while continuously acquiring FTIR spectra and monitoring the Newton rings in Fig. 1(a) to ensure parallelism.

Once the target thickness is reached (typically within 30 min of preparing the solution), we begin a time point spectral series, acquiring spectra every 5 min. Cavity thicknesses greater than ~ 1 μm are generally stable over several hours (±1.2%); however, thinner cavities often start to drift after a few minutes and thus must be periodically adjusted to maintain constant thickness based on feedback from the mode energies in the FTIR spectra.

III. RESULTS

A. Bare reaction kinetics

Figure 2(a) shows a typical time point spectral series for the bulk aqueous KOCN solution acquired by periodically (over the span of ~ 35 h) removing several drops from the sample vial and placing them onto the surface of the ATR crystal. The crystal is washed off between measurements, and the ATR geometry ensures the same "path length" of the evanescent wave in each successive measurement.

The broad absorption peak at ~ 3300 cm^{-1} is due to the combined symmetric and asymmetric stretching modes of water, while the sharp peak at 2169 cm^{-1} marks the OCN stretching mode of the cyanate ion. The inset highlights the decrease in the latter peak over time, reflecting the slow disappearance of OCN^- due to its hydrolysis in solution.

Assuming a constant effective interaction length, L, for the evanescent wave in the ATR measurement, the absorbance of the OCN^- peak (A) is directly proportional to the cyanate ion concentration (C) and its decadic molar absorption coefficient (ε) via the Beer–Lambert law, $A = \varepsilon CL = -\log_{10}(T)$, where T is the fraction of light transmitted relative to the reference case with no cyanate ions present. Since there is a large excess of water, the reaction begins with pseudo-first order kinetics and the concentration decreases exponentially over time from its starting value, C_0, according to $C = C_0 \exp(-kt)$. Consequently, since $A/A_0 = C/C_0$, a plot of $\ln(A/A_0)$ in Fig. 2(b) should yield the reaction rate constant, k, from its slope.

Fitting the data (purple dashed line) yields $k = (1.3 \pm 0.8) \times 10^{-6}$ s^{-1}, which is roughly two times larger than that reported by Hiura *et al.*[20] but three times smaller than that reported in Ref. 35.

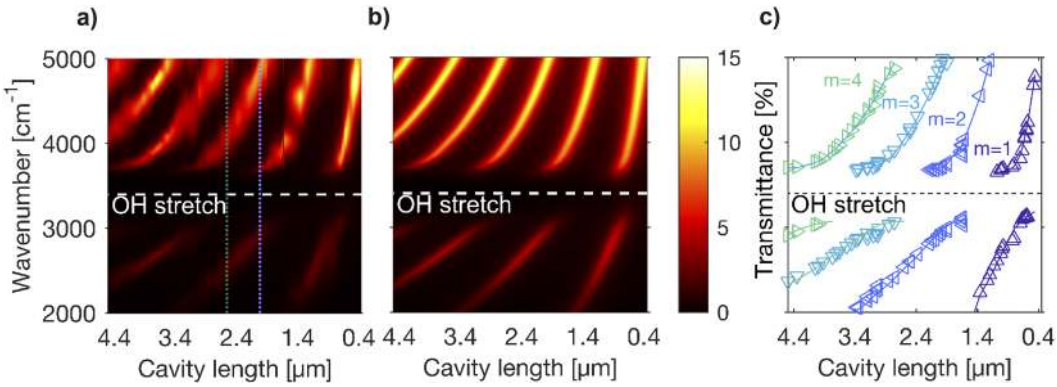

FIG. 3. (a) Transmission spectrum measured for a cavity filled with pure water over a thickness range of 0.4–4.4 μm. The green and purple vertical lines indicate the thicknesses at which the cavity kinetic measurements in Fig. 4 are carried out. (b) Transfer matrix simulation of the same system. (c) Polariton dispersion extracted from the peaks of the spectra in (a). Solid lines represent fits to the oscillator model described in the text, resulting in vacuum Rabi splittings of Ω = 800, 750, 740, and 740 cm^{-1} for the m = 1–4 cavity modes, respectively.

Differences in ambient temperature may contribute to the variation in these measurements (20 °C here vs 25 °C in Ref. 20 and 22 °C in Ref. 35) but cannot fully account for it as detailed in the supplementary material. Regardless, both control rates are clearly distinguished from the cavity-enhanced rate (denoted by the red dashed line) reported in Ref. 20.

B. VSC reaction kinetics

Despite its relatively broad linewidth, the strength of the collective OH stretching transition in water (peak absorption coefficient, $\alpha \approx 10^4$ cm^{-1} at $\nu = 3300$ cm^{-1}) readily facilitates VSC, as evident from the transmission spectra of a pure water cavity in Fig. 3(a). There, we observe anti-crossing behavior in the dispersion of the m = 1, 2, 3, and 4 modes when they become resonant with the OH stretch. The transfer matrix simulation in Fig. 3(b) reproduces these features, and Fig. 3(c) plots their dispersion based on the peak positions extracted from Fig. 3(a).

The dispersion is fit with a coupled oscillator model based on the complex frequency of the m^{th} cavity mode, $\tilde{\nu}_m = \nu_m - i\gamma_m$, where γ_m is the linewidth and $\nu_m = m/(2nd)$ is the real-valued resonance frequency set by the cavity thickness, d, and background refractive index, n. The interaction with a vibrational mode of complex frequency, $\tilde{\nu}_v = \nu_v - i\gamma_v$, is described by a 2 × 2 Hamiltonian,[36]

$$\hat{H} = \begin{bmatrix} \tilde{\nu}_m & V \\ V & \tilde{\nu}_v \end{bmatrix}, \tag{1}$$

in terms of the coupling strength, V. The eigenfrequencies of the coupled system are $\tilde{\nu}_\pm = (\tilde{\nu}_m + \tilde{\nu}_v)/2 \pm \sqrt{V^2 + (\tilde{\nu}_v - \tilde{\nu}_m)^2/4}$, and thus, the Rabi splitting between the upper and lower polariton branches is $\Omega = 2\sqrt{V^2 - (\gamma_v - \gamma_m)^2/4}$ at zero detuning when $\nu_m = \nu_v$. We note that this model assumes a Lorentzian absorber but remains a reasonable description for many organic microcavities with inhomogeneously broadened absorption lines like the OH stretch in Fig. 2(a).[36–38]

Fitting the data in Fig. 3(c), we obtain Rabi splittings that range from $\Omega = 800 \pm 20$ cm^{-1} for the m = 1 mode to $\Omega = 740 \pm 20$ cm^{-1} for the m = 4 mode. In all cases, the splitting exceeds the uncoupled linewidths of the system ($\gamma_v \sim 400$ cm^{-1} with $\gamma_m \sim 550$ cm^{-1} and $\gamma_m \sim 150$ cm^{-1} for the m = 1 and m = 4 modes, respectively) and is a substantial fraction of the bare transition frequency ($\Omega/2\nu_v = 0.12 > 0.10$), placing this system squarely in the vibrational ultrastrong coupling regime.[39] These results are in good agreement with Ref. 20.

The dispersion is similar when the cavity is filled with KOCN solution as shown in Fig. 4(a). However, upon setting the cavity length to $d = 2.02$ μm (zero detuning with the OH stretch) and carrying out a time point series on the OCN^- peak, we observe no difference from either the ATR reference or the rate in the same cavity upon detuning it to $d = 2.56$ μm after the first hour [see Fig. 4(b)]. Indeed, on the timescale of this experiment, no change in the OCN^- absorbance peak is detectable. These results are representative of multiple measurement attempts made on different days for run times of 1–3 h using sapphire, CaF_2, and ZnSe cavities; see the supplementary material for details.

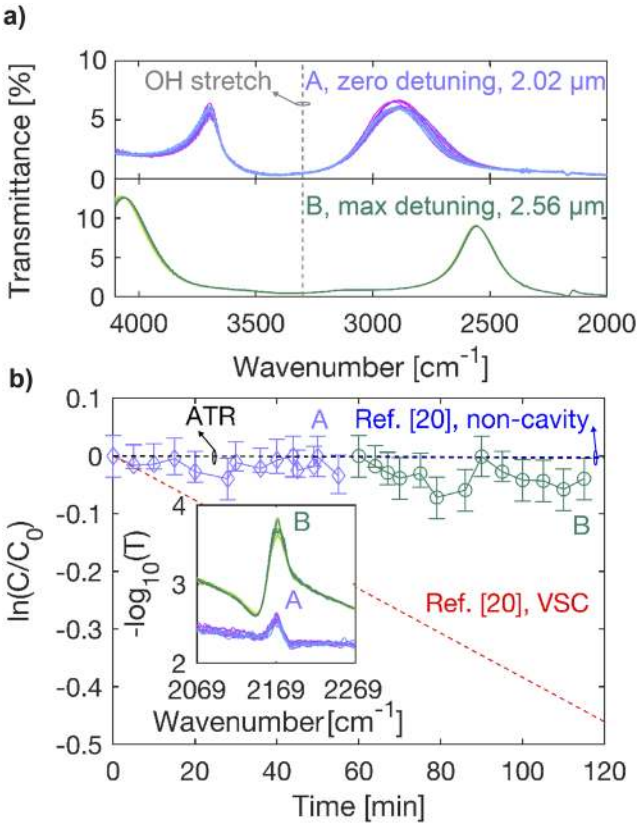

FIG. 4. (a) Time point transmission spectra acquired over the course of 2 h for a cavity filled with 2 mol/l aqueous KOCN solution. The cavity thickness is held at $d = 2.02$ μm (zero detuning for the $m = 2$ cavity mode, purple curves) for the first hour and is then increased to $d = 2.56$ μm (maximum detuning for the $m = 2$ cavity mode, green curves) during the second hour. The gray dashed line marks the OH stretching vibration at 3300 cm^{-1}. (b) Time point variation of the OCN^- absorbance peak as the cavity thickness is adjusted from zero detuning for $m = 2$ in the first hour [*A*, purple spectra in (a)] of the experiment to maximum detuning for $m = 2$ [*B*, green spectra in (a)] in the second hour. The black, blue, and red dashed lines indicate the ATR reference rate from Fig. 2(b), the non-cavity reference rate from Ref. 20, and the cavity VSC rate from Ref. 20, respectively. The inset shows the apparent absorbance, $A = -\log_{10}(T)$, of the OCN^- peak, which is the basis for the concentration ratio axis of the main plot.

IV. DISCUSSION

Although the time interval of the cavity experiment is not long enough to capture any change in OCN^- absorbance at its natural hydrolysis rate established in Fig. 2(b), achieving the 100-fold VSC rate enhancement reported by Hiura *et al.*[20] should have produced a clearly resolvable change per the dashed red line in Fig. 4(b). We emphasize that the main point of comparison is not with the ATR reference from Fig. 2 but between the on- and off-resonance data collected in the same cavity during the same experiment in Fig. 4 (datasets A and B, respectively). Statistically, the likelihood of there being *any* difference in the slope between these datasets is less than 60%; the chance of a ten-fold difference (as observed for different cavity conditions in Ref. 20) is less than one in a million.

The reason for the disagreement between our observations here and those in Ref. 20 is unclear, given that the cavities nominally share the same Au/SiO_2 mirror composition. The primary difference between the two setups is that the cavities in Ref. 20 are sealed with a Teflon spacer between the mirrors, whereas we use open cavities to permit piezoelectric actuation. While our approach admittedly leaves open the possibility that OCN^- ions from the detuned edge region of the cavities (per the Newton rings in Fig. 1) could diffuse in toward the middle and skew a genuine cavity enhancement in the hydrolysis rate, the timescale associated with such diffusion ($t \sim l_D^2/D \sim 10$ h to diffuse $l_D \sim 1$ cm with a diffusion coefficient of $\sim 10^{-5}$ $cm^2\ s^{-1}$)[40] makes this explanation seem unlikely.

One general point of note, however, is that inferring the reaction rate from the change in absorbance in a reactant or a product inside vs outside of a cavity can be misleading to begin with. This point follows from the transmittance of a Fabry–Pérot cavity:[41]

$$T_{fp} = \frac{(1-R)^2 T_{\text{int}}}{(1-RT_{\text{int}})^2 + 4RT_{\text{int}}\ \sin(\phi)^2}, \tag{2}$$

where R is the mirror reflectance, 2ϕ is the round trip phase (including that of the mirrors), and $T_{\text{int}} = 10^{-A}$ is the single pass internal transmittance we desire to measure. If the reaction rate is calculated directly from the cavity transmission in the same manner as the non-cavity case [i.e., from the slope of $\ln(\log_{10}(T_{\text{fp}})/\log_{10}(T_{0,\text{fp}}))$] as it is in Fig. 4(b) and Ref. 20, the apparent rate, k', differs from the actual rate, k, according to

$$k' \approx k\left[\frac{A_0(1+2R\ \cos(2\phi)T_{0,\text{int}})}{A_0 - 2R\ \cos(2\phi)T_{0,\text{int}} - 2\log_{10}(1-R)}\right]. \tag{3}$$

For a typical mirror reflectance, $R \sim 0.8$, and starting OCN^- absorbance, $A_0 \sim 0.5$, the apparent rate ranges between 2× and 10× lower than the actual rate depending on the cavity phase. This happens because, as the absorbance changes, it also alters the optical field distribution in the cavity, which causes the actual amount of light absorbed (and reflected) to change at a different rate.

Notably, Eq. (3) only predicts an apparent rate lower than the actual rate and thus cannot explain the enhancement reported by Hiura *et al.*,[20] although we note a slow drift in the uncoupled cavity mode (k_3) during their experiment, which suggests that the cavity phase may be varying over time. These and other potential pitfalls that arise when trying to infer changes in the concentration based on absorption inside a cavity underscore the need for alternative, non-optical measures of VSC reaction progress. We note that the ATR measurement used to determine our own reference rate in this work is not immune from the type of problem underlying Eq. (3) (i.e., changing absorbance modifies the evanescent field decay length); however, the error in this case is much smaller, with a <5% difference between k and k' expected from transfer matrix modeling.

V. CONCLUSION

In summary, we have attempted and failed to reproduce the VSC-enhanced hydrolysis rate of cyanate ions reported in Ref. 20. This result does not necessarily refute the findings of that work, as there could be as-yet-unappreciated subtleties that determine when VSC-modified kinetics can be observed, particularly in light of the many other studies that have provided compelling evidence for polariton chemistry in the dark.[17–19,21,22] Our work does, however, argue for a broader effort within the community to independently reproduce more of these claims since they continue to be the source of much enthusiasm and speculation in the field.

SUPPLEMENTARY MATERIAL

See the supplementary material for the VSC kinetic experiments repeated using CaF_2 and ZnSe cavities and additional ATR control measurements of the bare OCN^- hydrolysis rate for different temperatures and solution concentrations.

ACKNOWLEDGMENTS

This work was supported, in part, by the Charles E. Kaufman Foundation and the DARPA under Grant No. D19AC00011.

DATA AVAILABILITY

The data that support the findings of this study are available from the corresponding author upon reasonable request.

REFERENCES

[1] R. F. Ribeiro, L. A. Martínez-Martínez, M. Du, J. Campos-Gonzalez-Angulo, and J. Yuen-Zhou, "Polariton chemistry: Controlling molecular dynamics with optical cavities," Chem. Sci. **9**, 6325–6339 (2018).
[2] J. Feist, J. Galego, and F. J. Garcia-Vidal, "Polariton chemistry with organic molecules," ACS Photonics **5**, 205–216 (2018).
[3] T. W. Ebbesen, "Hybrid light-matter states in a molecular and material science perspective," Acc. Chem. Res. **49**, 2403–2412 (2016).
[4] M. Hertzog, M. Wang, J. Mony, and K. Börjesson, "Strong light-matter interactions: A new direction within chemistry," Chem. Soc. Rev. **48**, 937–961 (2019).
[5] F. Herrera and J. Owrutsky, "Molecular polaritons for controlling chemistry with quantum optics," J. Chem. Phys. **152**, 100902 (2020).
[6] J. A. Hutchinson, T. Schwartz, C. Genet, E. Devaux, and T. W. Ebbesen, "Modifying chemical landscapes by coupling to vacuum fields," Angew. Chem., Int. Ed. **51**, 1592–1596 (2012).
[7] B. Munkhbat, M. Wersäll, D. G. Baranov, T. J. Antosiewicz, and T. Shegai, "Suppression of photo-oxidation of organic chromophores by strong coupling to plasmonic nanoantennas," Sci. Adv. **4**, eaas9552 (2018).
[8] B. Xiang, R. F. Ribeiro, Y. Li, A. D. Dunkelberger, B. K. Simpkins, J. Yuen-Zhou, and W. Xiong, "Manipulating optical nonlinearities of molecular polaritons by delocalization," Sci. Adv. **5**, eaax5196 (2019).
[9] D. Polak, R. Jayaprakash, T. P. Lyons, L. Á. Martínez-Martínez, A. Leventis, K. J. Fallon, H. Coulthard, D. G. Bossanyi, K. Georgiou, A. J. Petty II, J. Anthony, H. Bronstein, J. Yuen-Zhou, A. I. Tartakovskii, J. Clark, and A. J. Musser, "Manipulating molecules with strong coupling: Harvesting triplet excitons in organic exciton microcavities," Chem. Sci. **11**, 343–354 (2020).
[10] N. Krainova, A. J. Grede, D. Tsokkou, N. Banerji, and N. C. Giebink, "Polaron photoconductivity in the weak and strong light-matter coupling regime," Phys. Rev. Lett. **124**, 177401 (2020).
[11] F. C. Spano, "Optical microcavities enhance the exciton coherence length and eliminate vibronic coupling in J-aggregates," J. Chem. Phys. **142**, 184707 (2015).
[12] J. Galego, F. J. Garcia-Vidal, and J. Feist, "Suppressing photochemical reactions with quantized light fields," Nat. Commun. **7**, 13841 (2016).
[13] F. Herrera and F. C. Spano, "Cavity-controlled chemistry in molecular ensembles," Phys. Rev. Lett. **116**, 238301 (2016).

[14]L. A. Martínez-Martínez, M. Du, R. F. Ribeiro, S. Kéna-Cohen, and J. Yuen-Zhou, "Polariton-assisted singlet fission in acene aggregates," J. Phys. Chem. Lett. **9**, 1951–1957 (2018).
[15]M. Du, R. F. Ribeiro, and J. Yuen-Zhou, "Remote control of chemistry in optical cavities," Chem **5**, 1167–1181 (2019).
[16]C. Schäfer, M. Ruggenthaler, H. Appel, and A. Rubio, "Modification of excitation and charge transfer in cavity quantum-electrodynamical chemistry," Proc. Natl. Acad. Sci. U. S. A. **116**, 4883–4892 (2019).
[17]A. Thomas, J. George, A. Shalabney, M. Dryzhakov, S. J. Varma, J. Moran, T. Chervy, X. Zhong, E. Devaux, C. Genet, J. A. Hutchison, and T. W. Ebbesen, "Ground-state chemical reactivity under vibrational coupling to the vacuum electromagnetic field," Angew. Chem., Int. Ed. **55**, 11462–11466 (2016).
[18]A. Thomas, L. Lethuillier-Karl, K. Nagarajan, R. M. A. Vergauwe, J. George, T. Chervy, A. Shalabney, E. Devaux, C. Genet, J. Moran, and T. W. Ebbesen, "Tilting a ground-state reactivity landscape by vibrational strong coupling," Science **363**, 615–619 (2019).
[19]J. Lather, P. Bhatt, A. Thomas, T. W. Ebbesen, and J. George, "Cavity catalysis by cooperative vibrational strong coupling of reactant and solvent molecules," Angew. Chem., Int. Ed. **58**, 10635–10638 (2019).
[20]H. Hiura, A. Shalabney, and J. George, "Vacuum-field catalysis: Accelerated reactions by vibrational ultra strong coupling," chemRxiv:7234721 (2018).
[21]A. Thomas, A. Jayachandran, L. Lethuillier-Karl, R. Vergauwe, K. Nagarajan, E. Devaux, C. Genet, J. Moran, and T. W. Ebbesen, "Ground state chemistry under vibrational strong coupling: Dependence of thermodynamic parameters on the Rabi splitting energy," Nanophotonics **9**, 249–255 (2019).
[22]R. M. A. Vergauze, A. Thomas, K. Nagarajan, A. Shalabney, J. George, T. Chervy, M. Seidel, E. Devaux, V. Torbeev, and T. W. Ebbesen, "Modification of enzyme activity by vibrational strong coupling of water," Angew. Chem., Int. Ed. **58**, 15324–15328 (2019).
[23]C. Gonzalez-Ballestero, J. Feist, E. G. Badía, E. Moreno, and F. J. Garcia-Vidal, "Uncoupled dark states can inherit polaritonic properties," Phys. Rev. Lett. **117**, 156402 (2016).
[24]T. Botzung, D. Hagenmüller, S. Schütz, J. Dubail, G. Pupillo, and J. Schachenmayer, "Dark state semilocalization of quantum emitters in a cavity," Phys. Rev. B **102**, 144202 (2020).
[25]D. Sidler, C. Schäfer, M. Ruggenthaler, and A. Rubio, "Polaritonic chemistry: Collective strong coupling implies strong local modification of chemical properties," J. Phys. Chem. Lett. **12**, 508–516 (2020).
[26]J. A. Campos-Gonzalez-Angulo, R. F. Ribeiro, and J. Yuen-Zhou, "Resonant catalysis of thermally activated chemical reactions with vibrational polaritons," Nat. Commun. **10**, 4685 (2019).
[27]I. Vurgaftman, B. S. Simpkins, A. D. Dunkelberger, and J. C. Owrutsky, "Negligible effect of vibrational polaritons on chemical reaction rates via density of states pathway," J. Phys. Chem. Lett. **11**, 3557–3562 (2020).
[28]S. Kéna-Cohen and J. Yuen-Zhou, "Polariton chemistry: Action in the dark," ACS Cent. Sci. **5**, 386–388 (2019).
[29]T. E. Li, J. E. Subotnik, and A. Nitzan, "Cavity molecular dynamics simulations of liquid water under vibrational ultrastrong coupling," Proc. Natl. Acad. Sci. U. S. A. **117**, 18324–18331 (2020).
[30]T. E. Li, A. Nitzan, and J. E. Subotnik, "On the origin of ground-state vacuum-field catalysis: Equilibrium consideration," J. Chem. Phys. **152**, 234107 (2020).
[31]L. A. Martínez-Martínez, R. F. Ribeiro, J. Campos-González-Angulo, and J. Yuen-Zhou, "Can ultrastrong coupling change ground-state chemical reactions?," ACS Photonics **5**, 167–176 (2017).
[32]O. Kapon, R. Yitzhari, A. Palatnik, and Y. R. Tischler, "Vibrational strong light–matter coupling using a wavelength-tunable mid-infrared open microcavity," J. Phys. Chem. C **121**, 18845–18853 (2017).
[33]W. Chen, M. D. Thoreson, S. Ishii, A. V. Kildishev, and V. M. Shalaev, "Ultra-thin ultra-smooth and low-loss silver films on a germanium wetting layer," Opt. Express **18**, 5124–5134 (2010).
[34]E. Centurioni, "Generalized matrix method for calculation of internal light energy flux in mixed coherent and incoherent multilayers," Appl. Opt. **44**, 7532–7539 (2005).
[35]N. Wen and M. H. Brooker, "Rate constants for cyanate hydrolysis to urea: A Raman study," Can. J. Chem. **72**, 1099–1106 (1994).
[36]R. J. Holmes and S. R. Forrest, "Strong exciton–photon coupling in organic materials," Org. Electron. **8**, 77–93 (2007).
[37]S. Kéna-Cohen, S. A. Maier, and D. D. C. Bradley, "Ultrastrongly coupled exciton–polaritons in metal-clad organic semiconductor microcavities," Adv. Opt. Mater. **1**, 827–833 (2013).
[38]K. S. Daskalakis, S. A. Maier, R. Murray, and S. Kéna-Cohen, "Nonlinear interactions in an organic polariton condensate," Nat. Mater. **13**, 271–278 (2014).
[39]A. F. Kochum, A. Miranowicz, S. D. Liberato, S. Savasta, and F. Nori, "Ultrastrong coupling between light and matter," Nat. Rev. Phys. **1**, 19–40 (2019).
[40]E. L. Cussler, *Diffusion Mass Transfer in Fluid Systems*, 2nd ed. (Cambridge University Press, 1997).
[41]A. Yariv and P. Yeh, *Photonics*, 6th ed. (Oxford University Press, 2007).